Long-range interactions of hydrogen atoms in excited states. III. nS-$1S$ interactions for $n \geqslant 3$

C. M. Adhikari, V. Debierre, and U. D. Jentschura
Department of Physics, Missouri University of Science and Technology, Rolla, Missouri 65409-0640, USA
(Received 7 April 2017; published 5 September 2017)

The long-range interaction of excited neutral atoms has a number of interesting and surprising properties such as the prevalence of long-range oscillatory tails and the emergence of numerically large van der Waals C_6 coefficients. Furthermore, the energetically quasidegenerate nP states require special attention and lead to mathematical subtleties. Here we analyze the interaction of excited hydrogen atoms in nS states ($3 \leqslant n \leqslant 12$) with ground-state hydrogen atoms and find that the C_6 coefficients roughly grow with the fourth power of the principal quantum number and can reach values in excess of 240 000 (in atomic units) for states with $n = 12$. The nonretarded van der Waals result is relevant to the distance range $R \ll a_0/\alpha$, where a_0 is the Bohr radius and α is the fine-structure constant. The Casimir-Polder range encompasses the interatomic distance range $a_0/\alpha \ll R \ll \hbar c/\mathcal{L}$, where $\mathcal{L}$ is the Lamb shift energy. In this range, the contribution of quasidegenerate excited nP states remains nonretarded and competes with the $1/R^2$ and $1/R^4$ tails of the pole terms, which are generated by lower-lying mP states with $2 \leqslant m \leqslant n-1$, due to virtual resonant emission. The dominant pole terms are also analyzed in the Lamb shift range $R \gg \hbar c/\mathcal{L}$. The familiar $1/R^7$ asymptotics from the usual Casimir-Polder theory is found to be completely irrelevant for the analysis of excited-state interactions. The calculations are carried out to high precision using computer algebra in order to handle a large number of terms in intermediate steps of the calculation for highly excited states.

DOI: 10.1103/PhysRevA.96.032702

I. INTRODUCTION

In general, the analysis of long-range interactions among neutral atoms in excited states is less trivial than one would expect at first glance. This is true for hydrogen atoms (in excited S states), which form the basis of the current investigation, as much as any other atom. The reasons are threefold. First, we note the presence of quasidegenerate excited nP states, which are only displaced from the nS states by the Lamb shift or the fine structure [1]. Due to the long wavelength of the involved virtual transitions, the contribution of the quasidegenerate states remains nonretarded over wide distance ranges. Second, the presence of lower-lying virtual mP states with $m \leqslant n$ leads to both oscillatory energy shifts and distance-dependent corrections to the decay width of the excited state [2–4]. Third, for nS-$1S$ interactions, there is a *gerade-ungerade* mixing term that depends on the symmetry of the excited-state contributions to the two-atom wave function. The mixing term is numerically large for $2S$-$1S$ interactions [1,5]. The eigenstates of the total Hamiltonian are composed of coherent superpositions of nS-$1S$ and $1S$-nS states in the two-atom system.

Let us try to provide some background on these issues. We recently analyzed [1] the interaction of metastable $2S$ hydrogen atoms with ground-state atoms. A long-standing discrepancy regarding the numerical value of the van der Waals C_6 coefficient could be resolved and the mixing term was treated for $2S$-$1S$ interactions [1,5–7]. In [8] we analyzed $2S$-$2S$ interactions and determined the hyperfine-resolved eigenstates of the van der Waals interaction among the S-S, P-P, and S-P submanifolds of the $n = 2$ hydrogen states. The physically interesting oscillatory tails of van der Waals interactions involving excited states were recently discussed in Refs. [2,3,9]. The special role of quasidegenerate excited states was analyzed in [1]. All of these concepts are relevant to the current investigation.

Finally, we should mention that the numerical evaluation of the van der Waals C_6 coefficient for excited states demands the rather sophisticated use of recurrence relations in order to express the polarizability matrix elements in terms of hypergeometric functions. This phenomenon is familiar from Lamb shift calculations [10,11]. The numerical calculations lead to van der Waals C_6 coefficients that grow rapidly with the principal quantum number.

Throughout this article we work in SI MKSA units and keep all factors of $\hbar$ and c in the formulas. With this choice, we attempt to extend the accessibility of the presentation to two different communities, namely, the quantum electrodynamics community, which in general uses the natural unit system, and the atomic physics community, where the atomic unit system is canonically employed. In the former, one sets $\hbar = c = \epsilon_0 = 1$, the electron mass is denoted by m_e, and one has the relation $e^2 = 4\pi\alpha$. This unit system is used, e.g., in the investigation reported in Ref. [12] on relativistic corrections to the Casimir-Polder interaction. In the atomic unit system, one has $|e| = \hbar = m_e = 1$ and $4\pi\epsilon_0 = 1$. The speed of light, in the atomic unit system, is $c = 1/\alpha \approx 137.036$. This system of units is especially useful for the analysis of atomic properties without radiative corrections. As the subject of the current study lies in between the two mentioned fields of interest, we choose the SI MKSA unit system as the most appropriate reference frame for our calculations. The formulas do not become unnecessarily complex and can be evaluated with ease for any experimental application.

We organize this paper as follows. The problem is somewhat involved; after an orientation in Sec. II, we focus on the $3S$-$1S$ interaction in Sec. III. In Sec. III A we study the van der Waals range. The very-large-distance limit is discussed in Sec. III C (atomic distance larger than the wavelength of the Lamb shift transition). The intermediate Casimir-Polder range is discussed in Sec. III B. States with $4 \leqslant n \leqslant 12$ are analyzed

in Sec. IV. Numerical examples are discussed in Sec. V. We summarize in Sec. VI.

II. ORIENTATION

As we are not interested in the hyperfine structure of the excited nS state ($n \geqslant 3$), we may write the total Hamiltonian of the two-atom system as

$$H_{\rm total} = H_S + H_{\rm FS} + H_{\rm LS} + H_{\rm vdW}. \tag{1}$$

Here H_S is the Schrödinger Hamiltonian, while $H_{\rm FS}$ is the fine-structure Hamiltonian, which can be approximated as (see Chap. 34 of Ref. [13])

$$H_{\rm FS} = \sum_{i=A,B} \left[-\frac{\vec{p}_i^{\,4}}{8m_e^3c^2} + \frac{1}{2}\alpha\left(\frac{\hbar^2 g_s}{2m_e^2 c}\right)\frac{\vec{L}_i\cdot\vec{S}_i}{|\vec{r}_i|^3} + \frac{\hbar^3}{8m_e^2 c}4\pi\alpha\delta^{(3)}(\vec{r}_i)\right], \tag{2}$$

where m_e is the electron mass. The momenta of the two atomic electrons are denoted by $\vec{p}_i$ (here i runs over the atoms A and B) and the distance vectors $\vec{r}_i = \vec{x}_i - \vec{R}_i$ are the coordinates relative to the nuclei (the electron and nucleus coordinates are $\vec{x}_i$ and $\vec{R}_i$, respectively). The fine-structure constant is $\alpha \approx 1/137.036$ and the electronic g factor is $g_s \simeq 2.002\,319$. As van der Waals interactions are relevant only for neutral systems, we restrict the discussion to neutral hydrogen atoms (nuclear charge number $Z = 1$). In leading logarithmic approximations, the Lamb shift Hamiltonian is approximated by [14]

$$H_{\rm LS} = \sum_{i=A,B} \frac{4}{3}\alpha^2 m_e c^2 \left(\frac{\hbar}{m_e c}\right)^3 \ln(\alpha^{-2})\delta^{(3)}(\vec{r}_i). \tag{3}$$

From Eq. (6) of Ref. [1], we recall the van der Waals Hamiltonian

$$H_{\rm vdW} = \frac{e^2}{4\pi\epsilon_0}\frac{\vec{r}_A\cdot\vec{r}_B - 3(\vec{r}_A\cdot\hat{R})(\vec{r}_B\cdot\hat{R})}{R^3}, \tag{4}$$

where $\vec{R} = \vec{R}_A - \vec{R}_B$, $R = |\vec{R}|$, and $\hat{R} = \vec{R}/R$. We assume that the hierarchy

$$\langle H_{\rm vdW}\rangle \ll \langle H_{\rm LS}\rangle \ll \langle H_{\rm FS}\rangle \tag{5}$$

is fulfilled for the entire distance range relevant to the current investigation ($R \gtrsim 30a_0$).

We carefully distinguish different asymptotic regimes for the interatomic interaction. In the so-called van der Waals range of interatomic distances,

$$a_0 = \frac{\hbar}{\alpha m_e c} \ll R \ll \frac{\hbar}{\alpha^2 m_e c} = \frac{a_0}{\alpha}, \tag{6}$$

the interatomic distance R is much larger than the Bohr radius $a_0 = \hbar/\alpha m_e c$, but much smaller than the wavelength of a typical optical transition (of order a_0/α), and the interaction is of the usual R^{-6} functional form. This remains valid if one atom is in an excited nS state. In the so-called Casimir-Polder range

$$R \gg \frac{\hbar}{\alpha^2 m_e c} = \frac{a_0}{\alpha}, \tag{7}$$

the interatomic distance is much larger than the wavelength of an optical transition and the interaction of *ground-state* atoms has a R^{-7} functional form. For the long-range interaction involving excited metastable atoms, however, we have to distinguish a third range of very large interatomic distances

$$R \gg \frac{\hbar c}{\mathcal{L}}, \tag{8}$$

which we would like to refer to as the Lamb shift range (where $\mathcal{L}$ is a typical Lamb shift energy). Care is needed in the intermediate range

$$\frac{\hbar}{\alpha^2 m_e c} = \frac{a_0}{\alpha} \ll R \ll \frac{\hbar c}{\mathcal{L}}. \tag{9}$$

A further complication arises. The state with atom A in the excited state and atom B in the ground state, $|nS\rangle_A|1S\rangle_B$, is degenerate with respect to the state $|1S\rangle_A|nS\rangle_B$ with the quantum numbers reversed. While there is no direct first-order coupling between the states due to the van der Waals interaction, an off-diagonal term is obtained in second order. It is of the same order of magnitude as the diagonal term, i.e., the term with the same in and out states. The Hamiltonian matrix in the basis of the degenerate states $|nS\rangle_A|1S\rangle_B$ and $|1S\rangle_A|nS\rangle_B$ then has off-diagonal (exchange or mixing) terms of second order in the van der Waals interaction [1,5].

A. Formalism for the direct terms

For nS-$1S$ interactions, the long-range interaction energy is the sum of three terms, namely, (i) a Wick-rotated interaction integral involving the nondegenerate states of the excited atom, (ii) a Wick-rotated interaction with the quasidegenerate states of the excited atom, and (iii) the sum of pole terms, due to lower-lying mP states with $m \leqslant n-1$. For details of the derivations, see Refs. [1,4,9].

Here we restrict the discussion to the direct term and indicate the specific contributions; a summary of all contributing terms will be given in Sec. II C. The first contribution to the Wick-rotated term, involving nondegenerate states, is given as

$$\widetilde{\mathcal{W}}^{(\rm dir)}(R) = -\frac{\hbar}{\pi c^4 (4\pi\epsilon_0)^2}\int_0^\infty d\omega\,\widetilde{\alpha}_{nS}(i\omega)\alpha_{1S}(i\omega) \times e^{-2\omega R/c}\frac{\omega^4}{R^2}\left[1 + 2\left(\frac{c}{\omega R}\right) + 5\left(\frac{c}{\omega R}\right)^2 + 6\left(\frac{c}{\omega R}\right)^3 + 3\left(\frac{c}{\omega R}\right)^4\right]. \tag{10}$$

The nondegenerate contribution to the nS-state polarizability (denoted by a tilde) is given as

$$\widetilde{\alpha}_{nS}(\omega) = \widetilde{P}_{nS}(\omega) + \widetilde{P}_{nS}(-\omega), \tag{11a}$$

$$\widetilde{P}_{nS}(\omega) = \frac{1}{3}\sum_{m\neq n}\frac{\langle nS|\vec{d}|mP\rangle\cdot\langle mP|\vec{d}|nS\rangle}{E_m - E_{nS} + \hbar\omega - i\epsilon}. \tag{11b}$$

Here $\vec{d} = e\vec{r}$ is the dipole operator. The sum over m includes the continuum states and the sum over the magnetic quantum numbers of the virtual P states is implied. However, note the

restriction to nondegenerate states in the sum over virtual states ($m \neq n$). The ground-state polarizability is

$$\alpha_{1S}(\omega) = P_{1S}(\omega) + P_{1S}(-\omega), \tag{12a}$$

$$P_{1S}(\omega) = \frac{1}{3}\sum_m \frac{\langle nS|\vec{d}|mP\rangle\cdot\langle mP|\vec{d}|nS\rangle}{E_m - E_{2S} + \hbar\omega - i\epsilon}. \tag{12b}$$

The second Wick-rotated term, involving the degenerate states, is given as

$$\overline{\mathcal{W}}^{(\mathrm{dir})}(R) = -\frac{\hbar}{\pi c^4 (4\pi\epsilon_0)^2}\int_0^\infty d\omega\, \overline{\alpha}_{nS}(i\omega)\alpha_{1S}(i\omega) \times e^{-2\omega R/c}\frac{\omega^4}{R^2}\left[1 + 2\left(\frac{c}{\omega R}\right) + 5\left(\frac{c}{\omega R}\right)^2 + 6\left(\frac{c}{\omega R}\right)^3 + 3\left(\frac{c}{\omega R}\right)^4\right]. \tag{13}$$

Here the degenerate part of the polarizability involves the nP states, with the same principal quantum number as the reference state,

$$\overline{\alpha}_{nS}(\omega) = \overline{P}_{nS}(\omega) + \overline{P}_{nS}(-\omega), \tag{14a}$$

$$\overline{P}_{nS}(\omega) = \frac{1}{9}\frac{\langle nS|\vec{d}|nP\rangle\cdot\langle nP|\vec{d}|nS\rangle}{-\mathcal{L}_n + \hbar\omega - i\epsilon} + \frac{2}{9}\frac{\langle nS|\vec{d}|nP\rangle\cdot\langle nP|\vec{d}|nS\rangle}{\mathcal{F}_n + \hbar\omega - i\epsilon}, \tag{14b}$$

where $\mathcal{L}_n$ and $\mathcal{F}_n$ are the Lamb shift and fine-structure splittings between quasidegenerate levels with principal quantum number n. (We have previously denoted by $\mathcal{L}$ an energy commensurate with the Lamb shift energies $\mathcal{L}_n$ in the range $2 \leqslant n \leqslant 12$.) Explicitly,

$$\mathcal{L}_n = E(nS_{1/2}) - E(nP_{1/2}), \tag{15a}$$

$$\mathcal{F}_n = E(nP_{3/2}) - E(nS_{1/2}). \tag{15b}$$

Both the Lamb shift $\mathcal{L}_n$ and the fine-structure splitting $\mathcal{F}_n$ decrease approximately as $1/n^3$ as the principal quantum number n increases [15,16]. The pole term [4,9] due to energetically lower $|mP\rangle$ states ($m < n$) becomes

$$\mathcal{Q}^{(\mathrm{dir})}(R) = -\frac{2}{3(4\pi\epsilon_0)^2 R^6}\sum_{m<n}\langle nS|\vec{d}|mP\rangle\cdot\langle mP|\vec{d}|nS\rangle\alpha_{1S}\left(\frac{E_{mn}}{\hbar}\right) \times \exp\left(-\frac{2iE_{mn}R}{\hbar c}\right)\left[3 + 6i\frac{E_{mn}R}{\hbar c} - 5\left(\frac{E_{mn}R}{\hbar c}\right)^2 - 2i\left(\frac{E_{mn}R}{\hbar c}\right)^3 + \left(\frac{E_{mn}R}{\hbar c}\right)^4\right]. \tag{16}$$

The Schrödinger energy difference is

$$E_{mn} = -\frac{E_h}{2}\left(\frac{1}{m^2} - \frac{1}{n^2}\right), \tag{17}$$

where $E_h = \alpha^2 m_e c^2$ is the Hartree energy. The real part of the pole term energy shift is

$$\mathcal{P}^{(\mathrm{dir})}(R) = -\frac{2}{3(4\pi\epsilon_0)^2 R^6}\sum_{m<n}\langle nS|\vec{d}|mP\rangle\cdot\langle mP|\vec{d}|nS\rangle\alpha_{1S}\left(\frac{E_{mn}}{\hbar}\right) \times\left\{\cos\left(\frac{2E_{mn}R}{\hbar c}\right)\left[3 - 5\left(\frac{E_{mn}R}{\hbar c}\right)^2 + \left(\frac{E_{mn}R}{\hbar c}\right)^4\right] + \frac{2E_{mn}R}{\hbar c}\sin\left(\frac{2E_{mn}R}{\hbar c}\right)\left[3 - \left(\frac{E_{mn}R}{\hbar c}\right)^2\right]\right\}. \tag{18}$$

The corresponding width term $\Gamma^{(\mathrm{dir})}(R)$ is obtained from the relation

$$\mathcal{Q}^{(\mathrm{dir})}(R) = \mathcal{P}^{(\mathrm{dir})}(R) - \frac{i}{2}\Gamma^{(\mathrm{dir})}(R) \tag{19}$$

and reads

$$\Gamma^{(\mathrm{dir})}(R) = -\frac{4}{3(4\pi\epsilon_0)^2 R^6}\sum_{m<n}\langle nS|\vec{d}|mP\rangle\cdot\langle mP|\vec{d}|nS\rangle\alpha_{1S}\left(\frac{E_{mn}}{\hbar}\right) \times\left\{\sin\left(\frac{2E_{mn}R}{\hbar c}\right)\left[3 - 5\left(\frac{E_{mn}R}{\hbar c}\right)^2 + \left(\frac{E_{mn}R}{\hbar c}\right)^4\right] - \frac{2E_{mn}R}{\hbar c}\cos\left(\frac{2E_{mn}R}{\hbar c}\right)\left[3 - \left(\frac{E_{mn}R}{\hbar c}\right)^2\right]\right\}. \tag{20}$$

B. Formalism for the mixing terms

Just as for the direct term, we need to identify a nondegenerate contribution $\widetilde{\mathcal{W}}^{(\mathrm{mix})}(R)$ to the Wick-rotated term, a degenerate contribution $\overline{\mathcal{W}}^{(\mathrm{mix})}(R)$, and a pole term $\mathcal{P}^{(\mathrm{mix})}(R)$. The first Wick-rotated term, involving nondegenerate states, is given as

$$\widetilde{\mathcal{W}}^{(\mathrm{mix})}(R) = -\frac{\hbar}{\pi c^4 (4\pi\epsilon_0)^2}\int_0^\infty d\omega\, \widetilde{\alpha}_{n\underline{S}1S}(i\omega)\alpha_{n\underline{S}1S}(i\omega) \times e^{-2\omega R/c}\frac{\omega^4}{R^2}\left[1 + 2\left(\frac{c}{\omega R}\right) + 5\left(\frac{c}{\omega R}\right)^2 + 6\left(\frac{c}{\omega R}\right)^3 + 3\left(\frac{c}{\omega R}\right)^4\right]. \tag{21}$$

The mixed polarizabilities are given as

$$\widetilde{\alpha}_{n\underline{S}1S}(\omega) = \frac{1}{3}\sum_{m\neq n}\sum_{\pm}\frac{\langle nS|\vec{d}|mP\rangle\cdot\langle mP|\vec{d}|1S\rangle}{E_m - E_{nS} \pm \hbar\omega - i\epsilon}, \tag{22a}$$

$$\alpha_{n\underline{S}1S}(\omega) = \frac{1}{3}\sum_{m}\sum_{\pm}\frac{\langle nS|\vec{d}|mP\rangle\cdot\langle mP|\vec{d}|1S\rangle}{E_m - E_{1S} \pm \hbar\omega - i\epsilon}. \tag{22b}$$

Note the restriction to nondegenerate states ($m \neq n$) in the sum over virtual states, in the expression for $\widetilde{\alpha}_{n\underline{S}1S}(\omega)$. The second Wick-rotated term, involving the degenerate states, is given as

$$\overline{\mathcal{W}}^{(\mathrm{mix})}(R) = -\frac{\hbar}{\pi c^4 (4\pi\epsilon_0)^2}\int_0^\infty d\omega\, \overline{\alpha}_{\underline{nS}1S}(i\omega)\alpha_{n\underline{S}1\underline{S}}(i\omega) \times e^{-2\omega R/c}\frac{\omega^4}{R^2}\left[1+2\left(\frac{c}{\omega R}\right)+5\left(\frac{c}{\omega R}\right)^2 +6\left(\frac{c}{\omega R}\right)^3+3\left(\frac{c}{\omega R}\right)^4\right]. \tag{23}$$

Here the degenerate part of the polarizability involves the nP states, with the same principal quantum number as the reference state,

$$\overline{\alpha}_{\underline{nS}1S}(\omega) = \frac{1}{9}\frac{\langle nS|\vec{d}|nP\rangle\cdot\langle nP|\vec{d}|1S\rangle}{-\mathcal{L}_n+\hbar\omega-i\epsilon} + \frac{2}{9}\frac{\langle nS|\vec{d}|nP\rangle\cdot\langle nP|\vec{d}|1S\rangle}{\mathcal{F}_n+\hbar\omega-i\epsilon}. \tag{24}$$

The mixed pole term due to energetically lower $|mP\rangle$ states becomes

$$\mathcal{Q}^{(\mathrm{mix})}(R) = -\frac{2}{3(4\pi\epsilon_0)^2R^6}\sum_{m<n}\langle nS|\vec{d}|mP\rangle\cdot\langle mP|\vec{d}|1S\rangle\alpha_{n\underline{S}1\underline{S}}\left(\frac{E_{mn}}{\hbar}\right) \times\exp\left(-\frac{2iE_{mn}R}{\hbar c}\right)\left[3+6i\frac{E_{mn}R}{\hbar c}-5\left(\frac{E_{mn}R}{\hbar c}\right)^2 -2i\left(\frac{E_{mn}R}{\hbar c}\right)^3+\left(\frac{E_{mn}R}{\hbar c}\right)^4\right]. \tag{25}$$

The real part is

$$\mathcal{P}^{(\mathrm{mix})}(R) = -\frac{2}{3(4\pi\epsilon_0)^2R^6}\sum_{m<n}\langle nS|\vec{d}|mP\rangle\cdot\langle mP|\vec{d}|1S\rangle\alpha_{n\underline{S}1\underline{S}}\left(\frac{E_{mn}}{\hbar}\right) \times\left\{\cos\left(\frac{2E_{mn}R}{\hbar c}\right)\left[3-5\left(\frac{E_{mn}R}{\hbar c}\right)^2+\left(\frac{E_{mn}R}{\hbar c}\right)^4\right] +\frac{2E_{mn}R}{\hbar c}\sin\left(\frac{2E_{mn}R}{\hbar c}\right)\left[3-\left(\frac{E_{mn}R}{\hbar c}\right)^2\right]\right\}. \tag{26}$$

The corresponding width term $\Gamma^{(\mathrm{mix})}(R)$ is obtained from the relation

$$\mathcal{Q}^{(\mathrm{mix})}(R) = \mathcal{P}^{(\mathrm{mix})}(R) - \frac{i}{2}\Gamma^{(\mathrm{mix})}(R) \tag{27}$$

and reads

$$\Gamma^{(\mathrm{mix})}(R) = -\frac{4}{3(4\pi\epsilon_0)^2R^6}\sum_{m<n}\langle nS|\vec{d}|mP\rangle\cdot\langle mP|\vec{d}|1S\rangle\alpha_{n\underline{S}1\underline{S}}\left(\frac{E_{mn}}{\hbar}\right) \times\left\{\sin\left(\frac{2E_{mn}R}{\hbar c}\right)\left[3-5\left(\frac{E_{mn}R}{\hbar c}\right)^2+\left(\frac{E_{mn}R}{\hbar c}\right)^4\right] -\frac{2E_{mn}R}{\hbar c}\cos\left(\frac{2E_{mn}R}{\hbar c}\right)\left[3-\left(\frac{E_{mn}R}{\hbar c}\right)^2\right]\right\}. \tag{28}$$

C. Adding direct and mixed terms

Depending on the symmetry of the two-atom wave function, we have for the eigenenergies of the two-atom system [1,5]

$$E(R) = E^{(\mathrm{dir})}(R) \pm E^{(\mathrm{mix})}(R), \tag{29a}$$

$$E^{(\mathrm{dir})}(R) = \widetilde{\mathcal{W}}^{(\mathrm{dir})}(R) + \overline{\mathcal{W}}^{(\mathrm{dir})}(R) + \mathcal{Q}^{(\mathrm{dir})}(R), \tag{29b}$$

$$E^{(\mathrm{mix})}(R) = \widetilde{\mathcal{W}}^{(\mathrm{mix})}(R) + \overline{\mathcal{W}}^{(\mathrm{mix})}(R) + \mathcal{Q}^{(\mathrm{mix})}(R). \tag{29c}$$

For the real part of the interaction energy,

$$\mathrm{Re}E(R) = \mathrm{Re}E^{(\mathrm{dir})}(R) \pm \mathrm{Re}E^{(\mathrm{mix})}(R), \tag{30}$$

one has

$$\mathrm{Re}E^{(\mathrm{dir})}(R) = \mathcal{W}^{(\mathrm{dir})}(R) + \mathcal{P}^{(\mathrm{dir})}(R) = \widetilde{\mathcal{W}}^{(\mathrm{dir})}(R) + \overline{\mathcal{W}}^{(\mathrm{dir})}(R) + \mathcal{P}^{(\mathrm{dir})}(R), \tag{31a}$$

$$\mathrm{Re}E^{(\mathrm{mix})}(R) = \mathcal{W}^{(\mathrm{mix})}(R) + \mathcal{P}^{(\mathrm{mix})}(R) = \widetilde{\mathcal{W}}^{(\mathrm{mix})}(R) + \overline{\mathcal{W}}^{(\mathrm{mix})}(R) + \mathcal{P}^{(\mathrm{mix})}(R). \tag{31b}$$

The sign of the mixing term depends on the symmetry of the wave function of the two-atom system [5]. In the following we will concentrate on the real part of the energy shift and use the symbols $E(R)$ and $\mathrm{Re}E(R)$ synonymously for both the direct and the mixing terms.

III. THE 3S-1S INTERACTION

A. van der Waals range

In the van der Waals distance range (6),

$$a_0 \ll R \ll \frac{a_0}{\alpha}, \tag{32}$$

the interaction is nonretarded, and the interaction energy is well approximated by the form

$$E(R) \approx -\frac{C_6}{R^6} = -\frac{D_6 \pm M_6}{R^6}. \tag{33}$$

The van der Waals coefficient $C_6 = D_6 \pm M_6$ contains a direct term D_6 and a mixing coefficient M_6.

First, we focus on the direct term. According to Sec. II A, D_6 is the sum of a nondegenerate Wick-rotated term $\widetilde{D}_6$, a degenerate Wick-rotated term $\overline{D}_6$, and a pole contribution $D_6^{\mathcal{P}}$. One writes

$$D_6(3S;1S) = \widetilde{D}_6(3S;1S) + \overline{D}_6(3S;1S) + D_6^{\mathcal{P}}(3S;1S). \tag{34}$$

Let us start with the nondegenerate contribution

$$\widetilde{D}_6(3S;1S) = \frac{3}{\pi}\frac{\hbar}{(4\pi\epsilon_0)^2}\int_0^\infty d\omega\,\widetilde{\alpha}_{3S}(i\omega)\alpha_{1S}(i\omega), \tag{35}$$

where $\widetilde{\alpha}_{3S}(\omega)$ has been defined in Eq. (11a). For the $1S$ polarizability, the result was recently given in Eqs. (15), (27a), and (27b) of Ref. [1]. For the $3S$ state, one obtains the nondegenerate matrix element

$$\widetilde{P}_{3S}(\omega) = \frac{e^2a_0^2}{E_h}\left[\frac{54\tau^2}{(1-\tau)^8(1+\tau)^6}(15538\tau^{12}-2852\tau^{11} -13283\tau^{10}+2090\tau^9+2871\tau^8+40\tau^7-62\tau^6 -492\tau^5+128\tau^4+236\tau^3-95\tau^2-46\tau+23)\right.$$

$$+\frac{6912\tau^9}{(1-\tau)^8(1+\tau)^8}(-1+9\tau^2)(3-7\tau^2)^2 \times {}_2F_1\left(1,-3\tau,1-3\tau,\frac{(1-\tau)^2}{(1+\tau)^2}\right)-\frac{972\,\tau^2}{1-\tau^2}\Bigg],$$

$$\tau=\left(1+\frac{18\hbar\omega}{\alpha^2 m_e c^2}\right)^{-1/2}. \tag{36}$$

The virtual $3P$ state is excluded from the sum over states in Eq. (36) by the explicit subtraction of the term $972\tau^2/(1-\tau^2)=54E_h/\hbar\omega$. One can verify that the expression (36) is finite in the limit $\tau\to 1$, which is equivalent to vanishing photon energy $\omega\to 0$.

The polarizability $\widetilde{\alpha}_{3S}(\omega)$ is recovered according to Eq. (11a), namely,

$$\widetilde{\alpha}_{3S}(\omega)=\widetilde{P}_{3S}(\omega)+\widetilde{P}_{3S}(-\omega). \tag{37}$$

A numerical evaluation of Eq. (35) leads to the result

$$\widetilde{D}_6(3S;1S)=180.320\,073\,947E_h a_0^6. \tag{38}$$

The degenerate contribution to D_6 can be handled analytically. It reads

$$\overline{D}_6(3S;1S)=\frac{3}{\pi}\frac{\hbar}{(4\pi\epsilon_0)^2}\int_0^\infty d\omega\,\overline{\alpha}_{3S}(i\omega)\alpha_{1S}(0). \tag{39}$$

Using Eqs. (23) and (24) of Ref. [1], one easily obtains the result for $\overline{D}_6(3S;1S)$,

$$\overline{D}_6(3S;1S)=729E_h a_0^6. \tag{40}$$

In the calculation, one uses the well-known result

$$\alpha_{1S}(0)=\frac{9}{2}\frac{e^2a_0^2}{E_h} \tag{41}$$

for the static polarizability of hydrogen.

In the van der Waals range, the pole term given in Eq. (18) can be approximated as

$$\mathcal{P}^{(\mathrm{dir})}(R) \approx -\frac{2}{(4\pi\epsilon_0)^2R^6}\sum_{m<n}\langle nS|\vec{d}|mP\rangle\cdot\langle mP|\vec{d}|nS\rangle\alpha_{1S}\left(\frac{E_{mn}}{\hbar}\right), \tag{42}$$

in view of the fact that $E_{mn}R/\hbar c\sim\alpha R/a_0\to 0$. For the $3S$-$1S$ interaction, this implies that the pole term yields another nontrivial contribution to D_6, which can be expressed as

$$D_6^{\mathcal{P}}(3S;1S)=\frac{2}{(4\pi\epsilon_0)^2}\langle 3S|\vec{d}|2P\rangle\cdot\langle 2P|\vec{d}|3S\rangle \times\alpha_{1S}\left(\omega=\frac{E_{2P3S}}{\hbar}\right), \tag{43}$$

where the sum over magnetic projections of the virtual $2P$ state is implied,

$$|\langle 3S|\vec{d}|2P\rangle|^2=\frac{2^{15}\times 3^8}{5^{12}}e^2a_0^2. \tag{44}$$

The polarizability $\alpha_{1S}(\omega=E_{2P3S}/\hbar)$ slightly differs from the static value given in Eq. (41),

$$\alpha_{1S}\left(\omega=\frac{E_{2P3S}}{\hbar}\right)=4.632\,338\,310\frac{e^2a_0^2}{E_h}. \tag{45}$$

Thus, the direct pole term $D_6^{\mathcal{P}}(3S;1S)$ is given by

$$D_6^{\mathcal{P}}(3S;1S)=8.158\,497\,516E_h a_0^6. \tag{46}$$

Adding the results from Eqs. (38), (40), and (46), one finally obtains the complete result for the D_6 coefficient of the $3S$-$1S$ interaction,

$$D_6(3S;1S)=\widetilde{D}_6(3S;1S)+\overline{D}_6(3S;1S)+D_6^{\mathcal{P}}(3S;1S) =917.478\,571\,464E_h a_0^6. \tag{47}$$

We have verified the result (47) by two alternative numerical methods. A discrete lattice representation of the radial Schrödinger equation and its spectrum [17] can be used in order to approximate the radial component of the Schrödinger-Coulomb propagator. This leads to an alternative evaluation of the D_6 coefficient in terms of an explicit sum over virtual states comprising the pseudospectrum (see Ref. [6]). The result confirms that $D_6(3S;1S)=917.478(1)$. Another possibility to verify the result (47) consists in an approach based on "intermediate quantum numbers", as outlined in the text surrounding Eq. (33) of Ref. [1]. The basic idea is that one can shift the reference-state quantum numbers artificially in the integrals describing the van der Waals energy, provided the bound-state energies of both involved states combined add up to the same total reference-state energy in the two-atom system. This second approach also confirms the result (47).

Similarly, the mixing term M_6 is obtained as the sum of a Wick-rotated nondegenerate term $\widetilde{M}_6(3S;1S)$, a Wick-rotated degenerate contribution $\overline{M}_6(3S;1S)$, and a pole term $M_6^{\mathcal{P}}(3S;1S)$,

$$M_6(3S;1S)=\widetilde{M}_6(3S;1S)+\overline{M}_6(3S;1S)+M_6^{\mathcal{P}}(3S;1S). \tag{48}$$

The nondegenerate Wick-rotated contribution

$$\widetilde{M}_6(3S;1S)=\frac{3}{\pi}\frac{\hbar}{(4\pi\epsilon_0)^2}\int_0^\infty d\omega\,\widetilde{\alpha}_{3S\underline{1S}}(i\omega)\alpha_{3S\underline{1S}}(i\omega) \tag{49}$$

is evaluated numerically, which yields

$$\widetilde{M}_6(3S;1S)=-5.588\,159\,518E_h a_0^6. \tag{50}$$

The degenerate coefficient $\overline{M}_6(3S;1S)$ is given by

$$\overline{M}_6(3S;1S)=\frac{3}{\pi}\frac{\hbar}{(4\pi\epsilon_0)^2}\int_0^\infty d\omega\,\overline{\alpha}_{3\underline{S}1S}(i\omega)\alpha_{3S\underline{1S}}(0), \tag{51}$$

where we refer to Eq. (24) for the definition of $\overline{\alpha}_{3\underline{S}1S}(\omega)$. We first carry out the integration and then take the limits $\mathcal{L}_3\to 0$ and $\mathcal{F}_3\to 0$ at the end of the calculation. The product of the matrix element of the dipole moment operators (with the sum over the magnetic projections implied) is

$$\langle 1S|\vec{d}|3P\rangle\cdot\langle 3P|\vec{d}|3S\rangle=-\frac{243\sqrt{3}e^2a_0^2}{64}. \tag{52}$$

The mixed static polarizability $\alpha_{3S\underline{1S}}(0)$ is given by

$$\alpha_{3S\underline{1S}}(0)=-\frac{621\sqrt{3}e^2a_0^2}{512E_h}. \tag{53}$$

An analytic calculation of the integral in Eq. (51) thus gives the result

$$\overline{M}_6(3S;1S) = \frac{3^9 \times 23}{2^{15}} E_h a_0^6 = 13.815\,582\,275 E_h a_0^6. \quad (54)$$

Similar to the direct pole term, the mixing pole term $M_6^{\mathcal{P}}(3S;1S)$ is given by

$$\begin{aligned} M_6^{\mathcal{P}}(3S;1S) &= \frac{2}{(4\pi\epsilon_0)^2} \langle 1S|\vec{d}|2P\rangle \cdot \langle 2P|\vec{d}|3S\rangle \\ &\quad \times \alpha_{3S\underline{1S}}\left(\omega = \frac{E_{2P3S}}{\hbar}\right) \\ &= \frac{2}{(4\pi\epsilon_0)^2}(-2.159\,394\,993)\frac{e^2a_0^2}{E_h}\frac{2^{15}e^2a_0^2}{5^6\times\sqrt{3}} \\ &= -5.229\,153\,219 E_h a_0^6. \end{aligned} \quad (55)$$

Thus, the total mixing contribution $M_6(3S;1S)$ is

$$\begin{aligned} M_6(3S;1S) &= \widetilde{M}_6(3S;1S) + \overline{M}_6(3S;1S) + M_6^{\mathcal{P}}(3S;1S) \\ &= 2.998\,269\,538\, E_h a_0^6. \end{aligned} \quad (56)$$

While the direct and mixing coefficients are of the same order of magnitude for $2S$-$1S$ interactions (≈176.75 versus ≈27.98), they differ by two orders of magnitude in the case of the $3S$-$1S$ system.

B. Intermediate distance

In the intermediate range of interatomic distances

$$\frac{a_0}{\alpha} \ll R \ll \frac{\hbar c}{\mathcal{L}}, \quad (57)$$

the treatment becomes a little sophisticated. As far as $\widetilde{\mathcal{W}}$ is concerned, we are in the Casimir-Polder regime where the result is given by an R^{-7} interaction. However, we incur a contribution proportional to R^{-6} from the quasidegenerate $3P$ states, i.e., from $\overline{\mathcal{W}}$. This contribution competes with the oscillatory long-range tails from the pole terms, which eventually drop off only as $1/R^2$.

From the quasidegenerate states, using the approach outlined in Eqs. (23) and (24) of Ref. [1], one obtains

$$\overline{\mathcal{W}}^{(\mathrm{dir})}_{3S;1S}(R) = -\frac{\overline{D}_6(3S;1S)}{R^6} = -729 E_h \left(\frac{a_0}{R}\right)^6. \quad (58)$$

The Wick-rotated contribution to the interaction is thus still of the R^{-6} form, as it is in the van der Waals range, but the coefficient is reduced in magnitude as compared to Eq. (47). In the intermediate range, the nondegenerate contribution $\widetilde{\mathcal{W}}^{(\mathrm{dir})}_{3S;1S}(R)$ is much smaller than $\overline{\mathcal{W}}^{(\mathrm{dir})}_{3S;1S}(R)$; it follows a $1/R^7$ law.

Let us now look into the pole term contribution $\mathcal{P}^{(\mathrm{dir})}_{3S;1S}(R)$ in the Casimir-Polder range. The Wick rotation from the positive real axis onto the imaginary axis picks up two poles at $\omega = -E_{3P_{1/2},3S}/\hbar + i\epsilon = -\mathcal{L}_3 + i\epsilon$ and $\omega = -E_{2P,3S}/\hbar + i\epsilon$, which, respectively, are due to the presence of the quasidegenerate $3P_{1/2}$ level and the low-lying $2P$ level. The contribution of the quasidegenerate $3P_{1/2}$ level to the $1/R^6$ part of the pole term is already contained in Eq. (58); we observe that the $1/R^6$ term in Eq. (18) does not have additional factors of $E_{mn} \sim \mathcal{L}_3$ and is therefore not suppressed by the Lamb shift numerators. By contrast, the terms of order $1/R^4$ and $1/R^2$ in Eq. (18) from the pole term due to the $3P_{1/2}$ levels are suppressed by the very small energy factor in the numerators of Eq. (18) (proportional to $\mathcal{L}_3^2$ and $\mathcal{L}_3^4$, respectively). For simplicity, we treat the contribution of the $3P_{1/2}$ and $3P_{3/2}$ levels uniformly by assigning their contribution to the Wick-rotated term. This procedure follows the one adopted in Eqs. (45a), (45b), and (46) of Ref. [1].

Finally, the direct pole term for the $3S$-$1S$ system (contribution of the lower-lying $2P$ states) reads

$$\begin{aligned} \mathcal{P}^{(\mathrm{dir})}_{3S;1S}(R) &= -\frac{2^{15}\times 3^8}{5^{12}}\frac{E_h a_0^6}{R^6}\alpha^{\mathrm{dl}}_{1S}\left(\frac{5E_h}{72\hbar}\right) \\ &\quad \times \left\{\cos\left(\frac{5\alpha R}{36a_0}\right)\left[3 - 5\left(\frac{5\alpha R}{72a_0}\right)^2 + \left(\frac{5\alpha R}{72a_0}\right)^4\right]\right. \\ &\quad \left. + \frac{5\alpha R}{36a_0}\sin\left(\frac{5\alpha R}{36a_0}\right)\left[3 - \left(\frac{5\alpha R}{72a_0}\right)^2\right]\right\}. \end{aligned} \quad (59)$$

Here $\alpha^{\mathrm{dl}}_{1S}(\omega)$ is the dimensionless polarizability, which we define as

$$\alpha^{\mathrm{dl}}_{1S}(\omega) = \frac{E_h}{e^2a_0^2}\alpha_{1S}(\omega). \quad (60)$$

For clarity, we add that our dimensionless polarizability could otherwise be characterized as the numerical value of the atomic polarizability in atomic units.

The Wick-rotated part of the mixing term is the sum

$$\mathcal{W}^{(\mathrm{mix})}_{3S;1S}(R) = \widetilde{\mathcal{W}}^{(\mathrm{mix})}_{3S;1S}(R) + \overline{\mathcal{W}}^{(\mathrm{mix})}_{3S;1S}(R). \quad (61)$$

The nondegenerate part $\widetilde{\mathcal{W}}^{(\mathrm{mix})}_{3S;1S}(R)$ follows an R^{-7} power law, whereas the degenerate part $\overline{\mathcal{W}}^{(\mathrm{mix})}_{3S;1S}(R)$ is still proportional to R^{-6}. Thus, to a good approximation, we have

$$\mathcal{W}^{(\mathrm{mix})}_{3S;1S}(R) \approx \overline{\mathcal{W}}^{(\mathrm{mix})}_{3S;1S}(R) = -\frac{3^9\times 23}{2^{15}} E_h \left(\frac{a_0}{R}\right)^6 \quad (62)$$

in the intermediate distance range. The mixed pole term is obtained as

$$\begin{aligned} \mathcal{P}^{(\mathrm{mix})}_{3S;1S}(R) &= \frac{2^{15}\times\sqrt{3}}{3^2\times 5^6}\frac{E_h a_0^6}{R^6}\alpha^{\mathrm{dl}}_{3S\underline{1S}}\left(\frac{5E_h}{72\hbar}\right) \\ &\quad \times \left\{\cos\left(\frac{5\alpha R}{36a_0}\right)\left[3 - 5\left(\frac{5\alpha R}{72a_0}\right)^2 + \left(\frac{5\alpha R}{72a_0}\right)^4\right]\right. \\ &\quad \left. + \frac{5\alpha R}{36a_0}\sin\left(\frac{5\alpha R}{36a_0}\right)\left[3 - \left(\frac{5\alpha R}{72a_0}\right)^2\right]\right\}, \end{aligned} \quad (63)$$

where $\alpha^{\mathrm{dl}}_{3S\underline{1S}}$ represents the dimensionless mixed $\alpha_{3S\underline{1S}}$ polarizability, defined according to Eq. (22b).

C. Very large interatomic distance

We now discuss the regime

$$R \gg \frac{\hbar c}{\mathcal{L}}. \quad (64)$$

This range is irrelevant for interactions in the laboratory but not for interactions relevant to astrophysical processes [18,19]. Expressed in units of the Hartree energy E_h, the physical values

of the Lamb shift and fine structure energies are [15,16,20]

$$\mathcal{L}_3 = 4.78 \times 10^{-8} E_h, \tag{65a}$$

$$\mathcal{F}_3 = 4.46 \times 10^{-7} E_h \approx 10\mathcal{L}_3. \tag{65b}$$

The approximation (64) is valid in the region

$$R \gg \frac{\hbar c}{\mathcal{L}_3} = \frac{a_0}{\alpha}\frac{E_h}{\mathcal{L}_3} = 2.864 \times 10^9 a_0 = 0.1516 \text{ m}. \tag{66}$$

For very large interatomic separation $R \to \infty$, the integrands in Eqs. (10) and (13) are significantly damped by exponential damping in ω. For large R, we may thus carry out the following approximations in the integrands of the van der Waals energy [Eqs. (10) and (13)]:

$$\alpha_{3S}(\omega) \approx \alpha_{3S}(0) \approx \overline{\alpha}_{3S}(0), \quad \alpha_{1S}(\omega) \approx \alpha_{1S}(0). \tag{67}$$

The remaining integral is evaluated as

$$\text{Re}\frac{\hbar}{\pi c^4}\int_0^\infty d\omega\, e^{-2\omega R/c}\frac{\omega^4}{R^2}\left[1 + 2\frac{c}{\omega R} + 5\left(\frac{c}{\omega R}\right)^2 + 6\left(\frac{c}{\omega R}\right)^3 + 3\left(\frac{c}{\omega R}\right)^4\right] = \frac{23}{4\pi}\frac{\hbar c}{R^7}. \tag{68}$$

The interaction is known as the retarded Casimir-Polder interaction and is proportional to R^{-7}.

The dominant contribution to the static polarizability of the excited $3S$ state comes from the virtual $3P_{1/2}$ and $3P_{3/2}$ levels,

$$\overline{\alpha}_{3S}(0) = 2\overline{P}_{3S}(0) = 36e^2a_0^2\left(\frac{2}{\mathcal{F}_3} - \frac{1}{\mathcal{L}_3}\right). \tag{69}$$

From Eqs. (41), (68), and (69) we find that the large-distance limit of the Wick-rotated contribution to the $3S$-$1S$ interaction energy is positive (repulsive),

$$\mathcal{W}^{(\text{dir})}_{3S;1S}(R) \overset{R\to\infty}{=} \frac{1863}{2\pi\alpha}E_h\left(\frac{a_0}{R}\right)^7\left(\frac{E_h}{\mathcal{L}_3} - 2\frac{E_h}{\mathcal{F}_3}\right). \tag{70}$$

This interaction is valid only for very large interatomic distances given in Eq. (66).

The dominant term in the range (64) comes from the pole contribution in Eq. (59) and reads

$$\mathcal{P}^{(\text{dir})}_{3S;1S}(R) = -\frac{2^3}{5^8}\frac{\alpha^4 E_h}{\rho^2}\alpha^{\text{dl}}_{1S}\left(\frac{5E_h}{72\hbar}\right)\cos\left(\frac{5\alpha\rho}{36}\right), \tag{71}$$

where $\rho = R/a_0$. The pole term falls off as R^{-2} and dominates the interaction energy (see Fig. 1). We note the numerical identities

$$\frac{2^3}{5^8} = 2.048 \times 10^{-5}, \quad \alpha^{\text{dl}}_{1S}\left(\frac{5E_h}{72\hbar}\right) = 4.632\,34. \tag{72}$$

The coefficient multiplying the leading oscillatory $1/R^2$ term given in Eq. (71) thus is of order 10^{-4}; this is in contrast to the D_6 and $\overline{D}_6$ coefficients, which are of order 10^3 (in atomic units). The numerical coefficients are thus in part responsible for a certain suppression of the long-range tail, as evident (in the intermediate region) from Fig. 2. The same trend is observed for nD-$1S$ interactions [4].

We should supplement the result for the mixing term in the very-long-range limit (66). As far as the mixing type contribution to the Casimir-Polder term is concerned, the degenerate part dominates the nondegenerate one. One has

$$\mathcal{W}^{(\text{mix})}_{3S;1S}(R) \approx \overline{W}^{(\text{mix})}_{3S;1S}(R) = \frac{3^7 \times 23^2}{2^{16}}\frac{E_h}{\pi\alpha}\left(\frac{a_0}{R}\right)^7\left(\frac{E_h}{\mathcal{L}_3} - 2\frac{E_h}{\mathcal{F}_3}\right). \tag{73}$$

By contrast, the leading $1/R^2$ contribution to the mixing pole term reads [see Eq. (63)]

$$\mathcal{P}^{(\text{mix})}_{3S;1S}(R) = -\frac{2^3 \times \sqrt{3}}{3^{10} \times 5^2}\alpha^4 E_h\left(\frac{a_0}{R}\right)^2 \times \alpha^{\text{dl}}_{3S1\underline{S}}\left(\frac{5E_h}{72\hbar}\right)\cos\left(\frac{5\alpha R}{36a_0}\right) \tag{74}$$

and it dominates in the very-long-range limit [Eq. (66)].

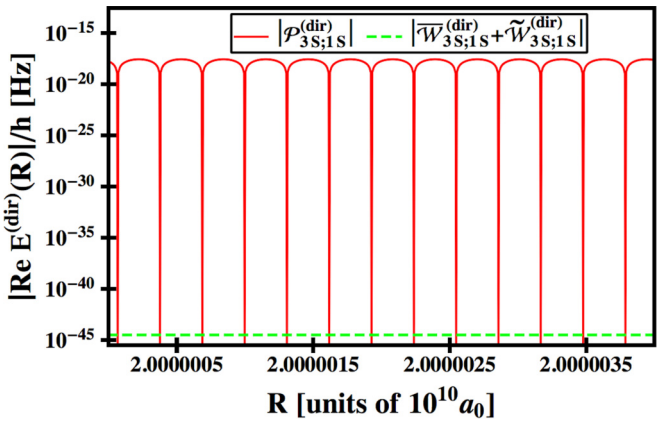

FIG. 1. Interaction energy in the $3S$-$1S$ system as a function of the interatomic distance R for a very long range. The pole term dominates over the Casimir-Polder term. However, the overall magnitude of the interaction is very small.

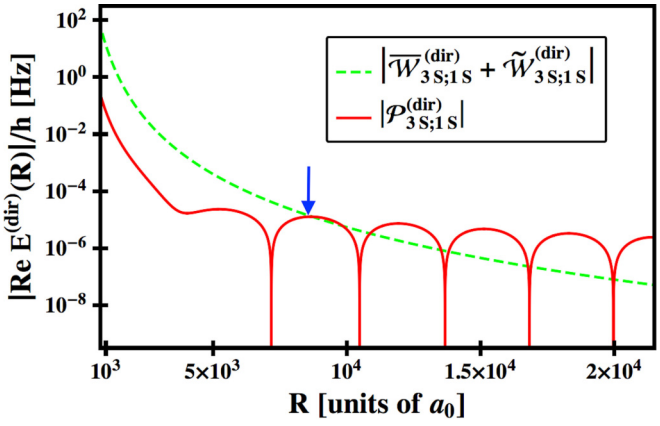

FIG. 2. Interaction energy in the $3S$-$1S$ system as a function of the interatomic distance R in the intermediate range. Initially, the Wick-rotated term dominates the pole term. As the interatomic distance increases, the pole term gradually dominates. The arrow indicates the position where the pole term becomes comparable to the Wick-rotated term. Note the logarithmic scale of the ordinate axis; the logarithm tends to $-\infty$ upon a sign change of the interaction energy.

TABLE I. Numerical values of the degenerate contributions $\overline{D}_6$, nondegenerate contributions $\widetilde{D}_6$, and the pole term contributions $D_6^{\mathcal{P}}$ to the direct D_6 van der Waals coefficients for two-atom systems in the van der Waals range. The coefficients are given in units of $E_h a_0^6$.

System	$\overline{D}_6$	$\widetilde{D}_6$	$D_6^{\mathcal{P}}$	$D_6 = \overline{D}_6 + \widetilde{D}_6 + D_6^{\mathcal{P}}$
$3S$-$1S$	729	180.320073947	8.158497516	917.478571464
$4S$-$1S$	2430	415.867781719	55.313793349	2901.174002323
$5S$-$1S$	6075	797.620619336	199.631309750	7072.251929086
$6S$-$1S$	$\frac{25515}{2}$	1361.858822274	526.146484053	14615.505306328
$7S$-$1S$	23814	2144.976599069	1146.872740254	27105.849339323
$8S$-$1S$	40824	3183.421765600	2200.822886660	46208.244652261
$9S$-$1S$	65610	4513.658548391	3854.012517378	73977.671065769
$10S$-$1S$	$\frac{200475}{2}$	6172.157501976	6299.459903847	112709.117405823
$11S$-$1S$	147015	8195.391734362	9757.185355911	164967.577090273
$12S$-$1S$	208494	10619.835391823	22062.734967733	241176.570359557

IV. STATES WITH $4 \leqslant n \leqslant 12$

A. van der Waals range

First, we discuss the nS-$1S$ interaction, with $4 \leqslant n \leqslant 12$, in the van der Waals regime (32),

$$a_0 \ll R \ll \frac{a_0}{\alpha}. \tag{75}$$

In this range, the interaction is described to a good approximation by the functional form (33). One should mention that the calculation of polarizability-type matrix elements that generalize Eq. (36) to states with $n \geqslant 4$ requires the sophisticated use of contiguous relations for hypergeometric functions [21,22]. Eventually, one can bring the matrix elements into a form that involves a rational function of the variable

$$\tau_n = \left(1 + \frac{n^2 \hbar\omega}{\alpha^2 m_e c^2}\right)^{1/2}, \tag{76}$$

where n is the principal quantum number, and a further term where a rational function of τ_n multiplies the hypergeometric function

$${}_2F_1\left(1, -n\tau_n, 1 - n\tau_n, \frac{(1-\tau_n)^2}{(1+\tau_n)^2}\right). \tag{77}$$

Here we describe calculations of the polarization-type matrix elements (11b) for nS states with principal quantum numbers as high as $n = 12$; several thousand terms are encountered in intermediate steps of the calculations; these are handled with the help of computer algebra systems [23]. For the mixed polarizabilities given in Eqs. (22a) and (22b), the calculations are even a little more involved because the radial wave functions of the bra and ket states are different; one may still express them in terms of a rational function of the τ_n variable and a hypergeometric function. Note that lattice methods that lead to a pseudospectrum of virtual states (see Ref. [17]) cannot be used with good effect for highly excited states because of numerical problems associated with the modeling of wave functions with many nodes. These numerical difficulties may be one reason why early numerical calculations for $C_6(2S;1S)$ coefficients [5,6] were never generalized to higher excited S states. Eventually, for $4 \leqslant n \leqslant 12$, the D_6 and M_6 coefficients are given in Tables I and II as the generalizations of Eqs. (47) and (56), respectively.

B. Intermediate distance

We discuss the intermediate distance range

$$\frac{a_0}{\alpha} \ll R \ll \frac{\hbar c}{\mathcal{L}}. \tag{78}$$

In Table II we generalize the result (58) and (62) to higher excited nS states. The nonretarded $1/R^6$ tail of the direct term has the functional form

$$\mathcal{W}^{(\mathrm{dir})}_{nS;1S}(R) = -\frac{\overline{D}_6(nS;1S)}{R^6}, \tag{79}$$

TABLE II. Numerical values of the degenerate contributions $\overline{M}_6$, nondegenerate contributions $\widetilde{M}_6$, and the pole term contributions $M_6^{\mathcal{P}}$ to the mixed M_6 van der Waals coefficients for two-atom systems in the van der Waals range. The coefficients are given in units of $E_h a_0^6$.

System	$\overline{M}_6$	$\widetilde{M}_6$	$M_6^{\mathcal{P}}$	$M_6 = \overline{M}_6 + \widetilde{M}_6 + M_6^{\mathcal{P}}$
$3S$-$1S$	13.815582275	−5.588159518	−5.229153219	2.998269538
$4S$-$1S$	8.015439766	−3.063629332	−4.033187464	0.918622970
$5S$-$1S$	5.716898855	−2.006704605	−3.302240659	0.407953591
$6S$-$1S$	4.480588908	−1.435991892	−2.825817540	0.218779478
$7S$-$1S$	3.702266657	−1.085159560	−2.485383226	0.131723872
$8S$-$1S$	3.163734811	−0.851710237	−2.224628639	0.087395934
$9S$-$1S$	2.767122768	−0.687554678	−2.020512545	0.059055545
$10S$-$1S$	2.461858057	−0.567328345	−1.851944579	0.042585133
$11S$-$1S$	2.219074417	−0.476448189	−1.711091985	0.031534242
$12S$-$1S$	2.021036738	−0.405984611	−1.590955009	0.024097118

TABLE III. Dimensionless dipole matrix elements F_{mn}. For given m, dipole matrix elements decrease with n. For given n, they grow with m. Most of the matrix elements are expressed in terms of their prime factors. Some of them are given as the approximate real numbers in order to save space in the table.

n \ m	2	3	4	5	6
3	$\frac{2^{15}\times 3^8}{5^{12}}$				
4	$\frac{2^{21}}{3^{15}}$	$\frac{2^{29}\times 3^7\times 13^2}{7^{16}}$			
5	$\frac{2^{15}\times 3^3\times 5^9}{7^{16}}$	$\frac{3^7\times 5^9\times 11^2}{2^{39}}$	$\frac{2^{22}\times 5^{10}\times 1447^2}{3^{39}}$		
6	$\frac{3^8}{2^{18}}$	$\frac{2^{20}\times 11^2}{3^{18}}$	$\frac{2^{19}\times 3^8\times 3329^2}{5^{23}}$	$\frac{2^{20}\times 3^8\times 5^7\times 67^2\times 14969^2}{11^{24}}$	
7	$\frac{2^{15}\times 5^8\times 7^9}{3^{41}}$	$\frac{2^3\times 3^7\times 7^9\times 23^2}{5^{22}}$	$\frac{5\times 2^{22}\times 3^5\times 7^9\times 31^2\times 233^2}{11^{24}}$	$\frac{5^7\times 7^9\times 8513^2}{2^{25}\times 3^{25}}$	$\frac{5\times 2^{15}\times 3^7\times 7^{10}\times 1289^2\times 104347^2}{13^{28}}$
8	$\frac{2^{30}\times 3^9}{5^{22}}$	$\frac{2^{38}\times 3^7\times 5^8\times 61^2}{11^{24}}$	$\frac{5\times 2^{25}\times 17^2}{3^{23}}$	$\frac{2^{38}\times 3^3\times 5^7\times 2549^2\times 3323^2}{13^{28}}$	$\frac{5\times 2^{30}\times 3^7\times 1051^2\times 14327^2}{7^{31}}$
9	$\frac{2^{15}\times 3^{17}\times 7^{12}}{11^{24}}$	$\frac{3^{11}\times 13^2}{2^{29}}$	$\frac{2^{22}\times 3^{17}\times 5^7\times 17^2\times 127^2\times 151^2}{13^{28}}$	$\frac{2^7\times 3^{17}\times 5^7\times 13^2\times 31^2\times 367^2}{7^{30}}$	$\frac{7\times 2^{15}\times 3^{11}\times 179^2\times 4451^2}{5^{31}}$
10	$\frac{2^{14}\times 5^9}{3^{27}}$	$\frac{2^{20}\times 3^7\times 5^9\times 7^{12}\times 97^2}{13^{28}}$	$\frac{2^{19}\times 3^{13}\times 5^{10}\times 709^2}{7^{30}}$	$\frac{2^{20}\times 5^2\times 73^2\times 167^2}{3^{33}}$	$\frac{3^7\times 5^{10}\times 7^3\times 10151^2}{2^{68}}$
11	$\frac{2^{15}\times 3^{31}\times 11^9}{13^{28}}$	$\frac{2^{25}\times 3^7\times 11^9\times 59^2}{7^{30}}$	$\frac{2^{22}\times 7^{12}\times 11^9\times 254083^2}{3^{31}\times 5^{33}}$	$\frac{3^{11}\times 5^7\times 11^9\times 368939^2}{2^{103}}$	$\frac{7\times 2^{15}\times 3^7\times 5^9\times 11^9\times 23^2\times 4391^2\times 109139^2}{17^{36}}$
12	$\frac{2^{21}\times 3^8\times 5^{18}}{7^{30}}$	$\frac{2^{29}\times 3^{18}\times 47^2}{5^{32}}$	$\frac{5\times 3^8\times 107^2}{2^{32}}$	$\frac{2^{29}\times 3^8\ 5^7\ 7^{12}\ 1237830047^2}{17^{36}}$	$\frac{5\times 7\times 2^{21}\ 23^2\ 1847^2}{3^{36}}$

n \ m	7	8	9	10	11
8	$\frac{2^{39}\times 7^7\times 61^2\times 7243^2\times 63689^2}{3^{29}\times 5^{32}}$				
9	$\frac{3^{17}\times 7^7\times 83^2\times 589910111^2}{2^{106}}$	389.637946068792			
10	10.168685073471	53.715308427324	632.560631964481		
11	4.646650394408	17.168247963601	86.059151181197	974.236212439363	
12	2.559407028125	7.772807970611	27.217069526272	131.078342047212	1438.320654775515

mainly due to the contribution from the degenerate nP states. The degenerate D_6 coefficient can be brought into the general form

$$\overline{D}_6(nS;1S) = \tfrac{81}{8}n^2(n^2-1)E_h a_0^6 \tag{80}$$

for $n \geqslant 2$. The leading contribution to the mixing term is

$$\mathcal{W}^{(\mathrm{mix})}_{nS;1S}(R) = -\frac{\overline{M}_6(nS;1S)}{R^6}, \tag{81}$$

again due to the contribution from the degenerate nP states. In the intermediate range, the Wick-rotated term of order $1/R^6$ competes with the pole term given in Eq. (18), due to lower-lying mP states. We express the latter as

$$\begin{aligned}\mathcal{P}^{(\mathrm{dir})}(R) &= -\frac{2E_h}{3\rho^6}\sum_{m=2}^{n-1}\frac{\langle nS|\vec{d}|mP\rangle\cdot\langle mP|\vec{d}|nS\rangle}{e^2a_0^2}\alpha^{\mathrm{dl}}_{1S}\left(\frac{d_{mn}\alpha E_h}{2\hbar}\right)\\ &\times\left\{\cos(d_{mn}\alpha\rho)\left[3-5\left(\frac{d_{mn}\alpha\rho}{2}\right)^2+\left(\frac{d_{mn}\alpha\rho}{2}\right)^4\right]\right.\\ &\left.+\,d_{mn}\alpha\rho\sin(d_{mn}\alpha\rho)\left[3-\left(\frac{d_{mn}\alpha\rho}{2}\right)^2\right]\right\},\end{aligned} \tag{82}$$

where $\rho = R/a_0$. We have used the identities

$$\frac{E_{mn}}{\hbar} = -\frac{d_{mn}\alpha E_h}{2\hbar}, \quad \frac{2E_{mn}R}{\hbar c} = -d_{mn}\alpha\rho, \tag{83}$$

where

$$d_{mn} \equiv \frac{1}{m^2}-\frac{1}{n^2}. \tag{84}$$

Values for the (dimensionless) dipole matrix elements

$$F_{mn} = \frac{\langle nS|\vec{d}|mP\rangle\cdot\langle mP|\vec{d}|nS\rangle}{e^2a_0^2}, \quad m<n,\ n\leqslant 12, \tag{85}$$

are given in Table III. While it is possible to give a semianalytic expression for the matrix elements (see the Appendix and Ref. [24]), these are quite complicated. It is instructive to have an explicit reference to the absolute magnitude of the coefficients; hence, we include Table III. The (dimensionless) polarizabilities

$$G_{mn} = \alpha^{\mathrm{dl}}_{1S}\left(\frac{d_{mn}\alpha E_h}{2\hbar}\right), \quad m<n,\ n\leqslant 12, \tag{86}$$

are given in Table IV for all states relevant to the current investigation. The real part of the mixing pole term has been given in Eq. (26),

$$\begin{aligned}\mathcal{P}^{(\mathrm{mix})}(R) &= -\frac{2E_h}{3\rho^6}\sum_{m<n}\frac{\langle nS|\vec{d}|mP\rangle\cdot\langle mP|\vec{d}|1S\rangle}{e^2a_0^2}\alpha^{\mathrm{dl}}_{nS\,1S}\left(\frac{d_{mn}\alpha E_h}{2\hbar}\right)\\ &\times\left\{\cos(d_{mn}\alpha\rho)\left[3-5\left(\frac{d_{mn}\alpha\rho}{2}\right)^2+\left(\frac{d_{mn}\alpha\rho}{2}\right)^4\right]\right.\\ &\left.+\,d_{mn}\alpha\rho\sin(d_{mn}\alpha\rho)\left[3-\left(\frac{d_{mn}\alpha\rho}{2}\right)^2\right]\right\}.\end{aligned} \tag{87}$$

TABLE IV. Numerical values of the dimensionless polarizabilities G_{mn}. The polarizability follows the following trends: It increases with the principal quantum number n of the reference state; for given n, the polarizability decreases with m and approaches the ground-state static value $9/2$ in the limit $m \to \infty$.

n \ m	2	3	4	5	6	7	8	9	10	11
3	4.632 34									
4	4.747 78	4.515 76								
5	4.815 70	4.533 88	4.503 37							
6	4.856 82	4.546 68	4.508 03	4.500 99						
7	4.883 15	4.555 41	4.511 81	4.502 55	4.500 36					
8	4.900 86	4.561 50	4.514 65	4.503 95	4.500 98	4.500 15				
9	4.913 31	4.565 87	4.516 79	4.505 09	4.501 58	4.500 43	4.500 07			
10	4.922 36	4.569 09	4.518 40	4.505 99	4.502 10	4.500 72	4.500 21	4.500 04		
11	4.929 13	4.571 52	4.519 64	4.506 70	4.502 53	4.500 98	4.500 36	4.500 11	4.500 02	
12	4.934 34	4.573 40	4.520 61	4.507 27	4.502 89	4.501 21	4.500 50	4.500 19	4.500 06	4.500 01

Numerical values for the (dimensionless) dipole matrix elements

$$H_{mn} = \frac{\langle nS|\vec{d}|mP\rangle \cdot \langle mP|\vec{d}|1S\rangle}{e^2 a_0^2}, \quad m < n,\ n \leqslant 12, \tag{88}$$

and the (dimensionless) polarizabilities

$$I_{mn} = \alpha^{\rm dl}_{n\underline{S}1\underline{S}}\left(\frac{d_{mn}\alpha E_h}{2\hbar}\right), \quad m < n,\ n \leqslant 12, \tag{89}$$

are given in Tables V and VI, respectively. For a discussion of the evaluation of the H_{mn}, see the Appendix. As the principal quantum number n of the excited state of the hydrogen atom interacting with the ground state increases, it takes longer and longer for the pole term to finally assume dominance over the Wick-rotated term (see Figs. 3–5).

A few words on the precise formulation of the intermediate distance range are perhaps in order. Namely, in principle, one might argue that the intermediate range should be bounded from above by $\hbar c/\mathcal{F}_n$, instead of $\hbar c/\mathcal{L}_n$, as the former quantity is smaller than the latter. In the rather narrow window where $\hbar c/\mathcal{F}_n < R < \hbar c/\mathcal{L}_n$, transitions between nS and $nP_{3/2}$ states are suppressed by retardation while those between nS and $nP_{1/2}$ states are not. We do not enter the details of this regime due to its narrow character, which would make it difficult to reliably clarify the asymptotic behavior of the interaction energy. Mathematically speaking, the inequality $R \ll \hbar c/\mathcal{L}_n$ implies $R \ll \hbar c/\mathcal{F}_n$ because $\mathcal{F}_n$ and $\mathcal{L}_n$ are apart by only a

TABLE V. Dimensionless dipole matrix elements H_{mn}. For given m, the dipole matrix elements decrease with the reference state quantum number n. Most of the matrix elements are presented in terms of their prime factor decompositions. Some of them are given as approximate real numbers in order to save some space in the table.

n \ m	2	3	4	5	6
3	$\frac{2^{15}}{5^6\times 3^{1/2}}$				
4	$\frac{2^{18}}{3^{12}}$	$\frac{13\times 2^8\times 3^7}{7^8}$			
5	$\frac{2^{15}\times 5^{9/2}}{3^3\times 7^8}$	$\frac{11\times 3^7\times 5^{9/2}}{2^{26}}$	$\frac{1447\times 2^{22}}{3^{18}\times 5^{3/2}}$		
6	$\frac{1}{2^{3/2}3^{1/2}}$	$\frac{11\times 2^{7/2}}{3^{11/2}}$	$\frac{3329\times 2^{41/2}\times 3^{11/2}}{5^{18}}$	$\frac{67\times 14969\times 2^{23/2}\times 5^7}{3^{7/2}\times 11^{12}}$	
7	$\frac{2^{15}\times 5^4\times 7^{9/2}}{3^{25}}$	$\frac{23\times 3^7\times 7^{9/2}}{2^5\times 5^{11}}$	$\frac{31\times 233\times 2^{22}\times 3^4\times 7^{9/2}}{5^6\times 11^{12}}$	$\frac{8513\times 5^7\times 7^{9/2}}{2^{11}\times 3^{20}}$	$\frac{1289\times 104347\times 2^{15}\times 3^7\times 5^4}{7^{7/2}\times 13^{14}}$
8	$\frac{2^{45/2}}{5^{11}}$	$\frac{61\times 2^{25/2}\times 3^7\times 5^4}{11^{12}}$	$\frac{17\times 2^{47/2}}{3^{10}\times 5^6}$	$\frac{2549\times 3323\times 2^{41/2}\times 5^7}{3^6\times 13^{14}}$	$\frac{1051\times 14327\times 2^{45/2}\times 3^7\times 5^4}{7^{24}}$
9	$\frac{2^{15}\times 3^4\times 7^6}{11^{12}}$	$\frac{13\times 3^9}{2^{21}}$	$\frac{17\times 127\times 151\times 2^{22}\times 3^{10}}{5^3\times 13^{14}}$	$\frac{13\times 31\times 367\times 2^5\times 35^7}{7^{15}}$	$\frac{179\times 4451\times 2^{15}\times 3^9}{5^{12}\times 7^8}$
10	$\frac{2^{29/2}\times 5^{9/2}}{3^{18}}$	$\frac{97\times 2^{7/2}\times 3^7\times 5^{9/2}\times 7^6}{13^{14}}$	$\frac{709\times 2^{41/2}\times 3^8}{5^{3/2}\times 7^{15}}$	$\frac{73\times 167\times 2^{23/2}\times 5^{9/2}}{3^{24}}$	$\frac{10151\times 3^7\times 5^{17/2}}{2^{53/2}\times 7^7}$
11	$\frac{2^{15}\times 3^{11}\times 11^{9/2}}{13^{14}}$	$\frac{59\times 2^6\times 3^7\times 11^{9/2}}{7^{15}}$	$\frac{254083\times 2^{22}\times 7^6\times 11^{9/2}}{3^{14}\times 5^{23}}$	$\frac{368939\times 5^7\times 11^{9/2}}{2^{50}\times 3^2}$	$\frac{23\times 4391\times 109139\times 2^{15}\times 3^7\times 5^8\times 11^{9/2}}{7^8\times 17^{18}}$
12	$\frac{2^{18}\times 5^9}{3^{1/2}\times 7^{15}}$	$\frac{47\times 2^8\times 3^{25/2}}{5^{16}}$	$\frac{107\times 3^{11/2}}{2^5\times 5^6}$	$\frac{123783047\times 2^{16}\times 5^7\times 7^6}{3^{7/2}\times 17^{18}}$	$\frac{23\times 1847\times 2^{18}\times 5^4}{3^{29/2}\times 7^8}$

n \ m	7	8	9	10	11
8	1.818 659 585 095				
9	0.680 670 360 144	1.944 278 307 643			
10	0.387 187 449 739	0.721 899 672 793	2.063 501 367 283		
11	0.261 733 234 429	0.408 122 742 837	0.761 118 380 971	2.177 019 770 691	
12	0.194 248 892 826	0.274 610 271 380	0.428 030 151 135	0.798 538 222 524	2.285 469 435 260

TABLE VI. Numerical values of the dimensionless polarizabilities I_{mn}. In contrast to the dimensionless polarizabilities G_{mn}, the trend in the numerical data implies lower values of I_{mn} for higher excited reference states. Also, I_{mn} for given n decreases as the value of m increases.

n \ m	2	3	4	5	6	7	8	9	10	11
3	−2.159 39									
4	−1.181 40	−1.135 68								
5	−0.782 85	−0.749 72	−0.745 94							
6	−0.571 51	−0.546 45	−0.543 13	−0.542 52						
7	−0.442 47	−0.422 73	−0.419 92	−0.419 32	−0.419 17					
8	−0.356 43	−0.340 36	−0.337 98	−0.337 43	−0.337 28	−0.337 23				
9	−0.295 46	−0.282 06	−0.280 02	−0.279 53	−0.279 38	−0.279 33	−0.279 32			
10	−0.250 31	−0.238 91	−0.237 15	−0.236 71	−0.236 57	−0.236 52	−0.236 50	−0.236 50		
11	−0.215 54	−0.205 87	−0.204 32	−0.203 93	−0.203 80	−0.203 76	−0.203 74	−0.203 73	−0.203 73	
12	−0.188 50	−0.179 87	−0.178 50	−0.178 15	−0.178 04	−0.177 99	−0.177 98	−0.177 97	−0.177 96	−0.177 96

single order of magnitude [see Eq. (65)]. If desired, then the regime $\hbar c/\mathcal{F}_n < R < \hbar c/\mathcal{L}_n$ could only be accessed reliably by a numerical calculation.

C. Very large distances

The regime

$$R \gg \frac{\hbar c}{\mathcal{L}} \tag{90}$$

is characterized by two competing terms, a $1/R^7$ term from the Wick-rotated contribution and an oscillatory contribution from the pole term. In Table VII we give a generalization of (70) and (73) to higher excited S states,

$$\mathcal{W}^{(\mathrm{dir})}_{nS;1S}(R) = -\frac{D_7(nS;1S)}{R^7}. \tag{91}$$

The D_7 coefficients obey the relationship

$$D_7(nS;1S) = \frac{207}{16} n^2(n^2-1)\frac{a_0^7 E_h}{\alpha\pi}\left(-\frac{E_h}{\mathcal{L}_n} + 2\frac{E_h}{\mathcal{F}_n}\right). \tag{92}$$

The Wick-rotated contribution to the mixing term has the functional form

$$\mathcal{W}^{(\mathrm{mix})}_{nS;1S}(R) = -\frac{M_7(nS;1S)}{R^7}, \tag{93}$$

where we refer to Table VII for the numerical values. However, the $1/R^7$ tails are suppressed, in the very-long-range limit, in comparison to the pole terms, which go as $1/R^2$.

In fact, due to the trend in the numerical coefficients recorded in Tables III—VI, the dominant contributions from the pole terms (direct and mixing term) comes from virtual $2P$ states and can be expressed as

$$\mathcal{P}^{(\mathrm{dir})}(R) \approx -\frac{d_{2n}^4 E_h \alpha^4}{24\rho^2} F_{2n} G_{2n} \cos(d_{2n}\alpha\rho) \tag{94}$$

and

$$\mathcal{P}^{(\mathrm{mix})}(R) \approx -\frac{d_{2n}^4 E_h \alpha^4}{24\rho^2} H_{2n} I_{2n} \cos(d_{2n}\alpha\rho), \tag{95}$$

respectively. Contributions from mP states with $3 \leqslant m \leqslant n-1$ are numerically, but not parametrically, suppressed. The

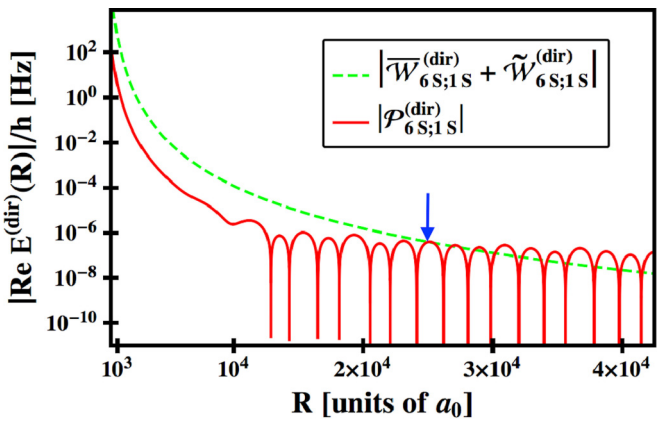

FIG. 3. Interaction energy in the $6S$-$1S$ system as a function of the interatomic distance R in the intermediate range. The smooth curve represents the absolute value of the total Wick-rotated contribution and the oscillatory curve gives the pole-type contribution. The arrow indicates the minimum value of R at which the Wick-rotated and pole terms are equal in magnitude.

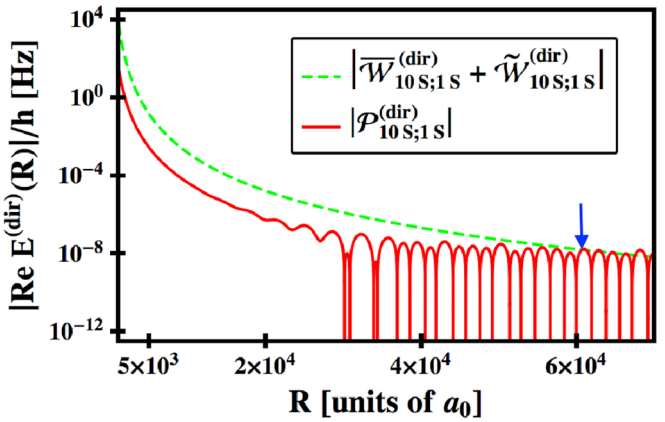

FIG. 4. Interaction energy in the $10S$-$1S$ system as a function of the interatomic distance R in the intermediate range. The smooth curve represents the absolute value of the total Wick-rotated contribution and the oscillatory curve gives the pole-type contribution. The arrow indicates the minimum value of R at which the Wick-rotated and pole terms are equal in magnitude.

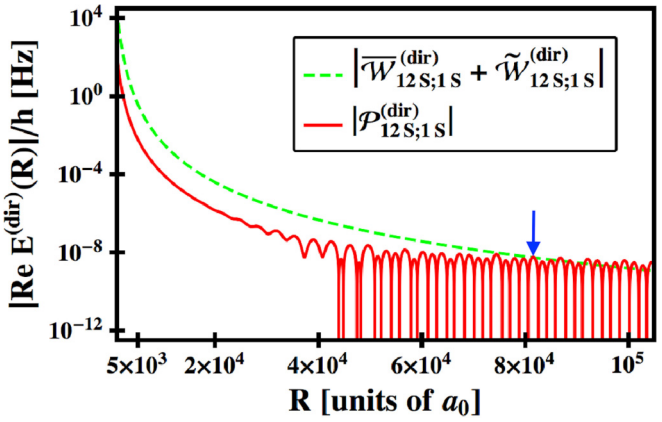

FIG. 5. Interaction energy in the $12S$-$1S$ system as a function of the interatomic distance R in the intermediate range. The smooth curve represents the absolute value of the total Wick-rotated contribution and the oscillatory curve gives the pole-type contribution. The arrow indicates the minimum value of R at which the Wick-rotated and pole terms are equal in magnitude.

quantity d_{mn} was defined in Eq. (84) and ρ was defined in the text following Eq. (71).

V. NUMERICAL EXAMPLES

It can be helpful to have numerical reference data available for the pole term, as well as the Wick-rotated contribution to the interaction energy, for sample values of the interatomic distance. These are given in Tables VIII and IX. We concentrate on the $3S$-$1S$ and $4S$-$1S$ systems. One can clearly discern the dominance of the pole term in the long-range limit and its suppression in the van der Waals range (6). Note that both the direct and the mixing terms are indicated in Tables VIII and IX. In entries with $\pm$, the positive sign refers to the *gerade* configuration of the wave functions and the negative sign is relevant to the *ungerade* configuration. The opposite happens for the numerical entries involving the $\mp$ sign.

TABLE VII. Numerical values of the degenerate contributions to the direct D_7 and mixed M_7 Casimir-Polder coefficients for two-atom systems. The coefficients are given in units of $\frac{1}{\alpha\pi}E_h^2(-\frac{1}{\mathcal{L}_n}+\frac{2}{\mathcal{F}_n})a_0^7$ (which is a negative quantity), explaining why the overall interaction term is repulsive.

System	D_7	M_7
$3S$-$1S$	$\frac{1863}{2}$	17.653 244 019
$4S$-$1S$	3105	10.241 950 813
$5S$-$1S$	$\frac{15\,525}{2}$	7.304 926 315
$6S$-$1S$	$\frac{65\,205}{4}$	5.725 196 938
$7S$-$1S$	30 429	4.730 674 062
$8S$-$1S$	52 164	4.042 550 036
$9S$-$1S$	83 835	3.535 767 981
$10S$-$1S$	$\frac{512\,325}{4}$	3.145 707 517
$11S$-$1S$	$\frac{375\,705}{2}$	2.835 483 977
$12S$-$1S$	266 409	2.582 435 832

TABLE VIII. Numerical values of the long-range interaction frequency shift in the $(3S;1S)$ system. The $\mathcal{W}_{3S;1S}(R)$ is the Wick-rotated-type frequency shift and the $\mathcal{P}_{3S;1S}(R)$ is the pole-type frequency shift. The $\pm$ sign corresponds to the $\pm$ sign in the $(|1S\rangle|3S\rangle \pm |3S\rangle|1S\rangle)$ superposition. For small separation, the Wick-rotated frequency is dominant, however, for large separation, the pole term dominates.

R (Å)	$\mathcal{W}_{3S;1S}(R)$ [Hz]	$\mathcal{P}_{3S;1S}(R)$ [Hz]
20	$-(2.053 \pm 0.019) \times 10^9$	$-(1.842 \mp 1.181) \times 10^7$
40	$-(3.207 \pm 0.029) \times 10^7$	$-(2.876 \mp 1.185) \times 10^5$
80	$-(5.007 \pm 0.045) \times 10^5$	$-(4.505 \mp 2.888) \times 10^3$
200	$-(2.045 \pm 0.019) \times 10^3$	$-(1.865 \mp 1.195) \times 10^1$
400	$-(3.174 \pm 0.030) \times 10^1$	$-(3.035 \mp 1.946) \times 10^{-1}$
800	$-(4.890 \pm 0.050) \times 10^{-1}$	$-(5.561 \mp 3.565) \times 10^{-3}$
2000	$-(2.328 \pm 0.012) \times 10^{-3}$	$-(9.460 \mp 2.021) \times 10^{-4}$
20 000	$-(1.714 \pm 0.029) \times 10^{-9}$	$-(1.835 \mp 0.392) \times 10^{-7}$
200 000	$-(1.653 \pm 0.031) \times 10^{-15}$	$-(4.032 \mp 0.862) \times 10^{-9}$

VI. CONCLUSION

We have studied nS-$1S$ van der Waals interactions among hydrogen atoms in detail, for $n \geqslant 3$. In a brief orientation in Sec. II, we discuss the nondegenerate Wick-rotated contribution $\widetilde{\mathcal{W}}(R)$, the degenerate term $\overline{\mathcal{W}}(R)$, and the pole term $\mathcal{Q}(R)$, which splits into a real energy shift $\mathcal{P}(R)$ and a width term $\Gamma(R)$. We treat the $3S$-$1S$ interaction in great detail in Sec. III before generalizing the approach to the nS-$1S$ case in Sec. IV ($4 \leqslant n \leqslant 12$). Numerical reference data are given in Sec. V. These numerical data are crucial in a reliable determination of pressure shifts in high-precision spectroscopy experiments involving highly excited S states [25,26].

We differentiate three distance ranges given in Eqs. (6)–(8), which we recall for convenience:

$$\frac{\hbar}{\alpha m_e c} \ll R \ll \frac{\hbar}{\alpha^2 m_e c} \quad \text{(van der Waals range)}, \tag{96a}$$

$$\frac{\hbar}{\alpha^2 m_e c} \ll R \ll \frac{\hbar c}{\mathcal{L}_n} \quad \text{(Casimir-Polder range)}, \tag{96b}$$

$$R \gg \frac{\hbar c}{\mathcal{L}_n} \quad \text{(Lamb shift range)}. \tag{96c}$$

TABLE IX. Numerical values of the Wick-rotated-type $\mathcal{W}_{4S;1S}(R)$ and the pole-type $\mathcal{P}_{4S;1S}(R)$ long-range interaction frequency shift in the $(4S;1S)$ system. The $\pm$ sign corresponds to the $\pm$ sign in the $(|1S\rangle|4S\rangle \pm |4S\rangle|1S\rangle)$ superposition.

R (Å)	$\mathcal{W}_{4S;1S}(R)$ [Hz]	$\mathcal{P}_{4S;1S}(R)$ [Hz]
20	$-(6.425 \pm 0.011) \times 10^9$	$-(1.249 \mp 0.091) \times 10^8$
40	$-(1.004 \pm 0.002) \times 10^8$	$-(1.951 \mp 0.146) \times 10^6$
80	$-(1.568 \pm 0.003) \times 10^6$	$-(3.048 \mp 0.229) \times 10^4$
200	$-(6.416 \pm 0.011) \times 10^3$	$-(1.246 \mp 0.094) \times 10^2$
400	$-(1.000 \pm 0.002) \times 10^2$	$-(1.936 \mp 0.151) \times 10^0$
800	$-(1.554 \pm 0.003) \times 10^0$	$-(2.962 \mp 0.256) \times 10^{-2}$
2000	$-(8.851 \pm 0.003) \times 10^{-3}$	$-(5.984 \mp 0.462) \times 10^{-3}$
20 000	$-(5.822 \pm 0.016) \times 10^{-9}$	$-(1.152 \mp 0.994) \times 10^{-6}$
200 000	$-(5.519 \pm 0.018) \times 10^{-15}$	$-(1.658 \mp 1.321) \times 10^{-8}$

In the van der Waals range, the interatomic interaction is described to good accuracy by a functional form $-C_6(A;B)/R^6$, where $C_6(A;B) = D_6(A;B) \pm M_6(A;B)$ is the van der Waals coefficient. The direct coefficient D_6 is the sum of a nondegenerate contribution $\widetilde{D}_6$, a degenerate contribution $\overline{D}_6$, and a pole term $D_6^{\mathcal{P}}$. Analogously, one has $M_6 = \widetilde{M}_6 + \overline{M}_6 + M_6^{\mathcal{P}}$, where $\widetilde{M}_6$ is the nondegenerate contribution to the mixing van der Waals coefficient, while $\overline{M}_6$ and $M_6^{\mathcal{P}}$ are the degenerate and pole term counterparts.

The main results reported in the present investigation can be summarized as follows. (i) The van der Waals coefficients for the direct and mixing terms have been obtained, for nS-$1S$ interactions, in Tables I and II, on the basis of rather involved analytic calculations of polarizability-type matrix elements [see Eq. (11b)], with several thousand terms in intermediate steps of the calculations; these were handled using computer algebra [23]. The data show a surprising trend: Namely, the D_6 and $\overline{D}_6$ coefficients, as a function of n, are consistent with an n^4 asymptotics for large n [see also Eq. (80)]. By contrast, the mixing coefficients M_6 and $\overline{M}_6$ tend to decrease with n. However, for small n (say, $n = 3$), in contrast to nD-$1S$ interactions [4], the M_6 and $\overline{M}_6$ coefficients for nS-$1S$ interactions, obtained here, can be comparatively large and smaller than D_6 and $\overline{D}_6$ by only one order of magnitude. This situation is completely different for nD-$1S$ interactions [4].

(ii) We carry out a detailed analysis of the oscillatory long-range tails of the van der Waals interaction for nS-$1S$ interactions. The results obtained for nS-$1S$ interactions indicate that the $1/R^2$ long-range tails are somewhat suppressed in comparison to the standard $1/R^6$ interaction, due to the smallness of the overall numerical factors multiplying the energy shifts. For example, for $3S$-$1S$ interactions, one should compare the overall prefactor in Eq. (59), which is

$$\frac{2^{15} \times 3^8}{5^{12}} \approx 0.880\,60, \tag{97}$$

with the magnitude of the D_6 coefficient given as $D_6 \approx 917.478$ according to Table I. We also refer to Eqs. (71) and (72) for the overall prefactors multiplying the oscillatory tail for the $3S$-$1S$ interaction. For $12S$-$1S$ interactions, the situation is even more extreme: The leading contribution to the pole term, as far as the energy difference E_{mn} is concerned, comes from a virtual $2P$ state; the overall coefficient in the pole term comes from Table I as

$$\frac{2^{21} \times 3^8 \times 5^{18}}{7^{30}} \approx 0.002\,33, \tag{98}$$

while the D_6 coefficient is as large as 241176 (see Table I). The difference by several orders of magnitude between the overall multiplying coefficients does not originate from a parametric suppression of the pole terms, but is exclusively due to the dependence of the transition energies and dipole transition matrix elements on the quantum numbers of the involved states. The trend of the coefficients has the following consequences for the physical nature of the interaction: In the intermediate range, the nonretarded quasidegenerate $1/R^6$ contributions to $\overline{D}_6$ and $\overline{M}_6$ compete with the oscillatory long-range tail of the $1/R^2$ pole term (see Figs. 2–5). As the principal quantum number increases, it takes longer and longer for the pole term to assume dominance over the nonretarded tail of the van der Waals interaction, with the latter being given in Eq. (80).

(iii) The analysis presented here also raises interesting further questions. For example, for nS-$1S$ interactions, the oscillatory cosine terms, proportional to R^{-2}, eventually dominate in the long-range limit [see Eqs. (94) and (95)] and the Casimir-Polder tail of order R^{-7} is found to be phenomenologically irrelevant for interactions involving higher excited states. Based on a parametric analysis, one might think that the R^{-2} oscillatory tails should also dominate over the R^{-6} van der Waals interactions in the intermediate range of interatomic distances. However, as evident from Figs. 2–5, the dominance sets in only after the absolute magnitude of the energy shift has decreased to well below 1 Hz in frequency units. As already stated, one can attempt to justify this trend based on the dependence of the energy differences d_{mn} on the principal quantum numbers. For example, one has $d_{(n-1)n} \sim n^{-3}$ and the fact that d_{mn} enters the leading R^{-2} contribution to the pole term in the fourth power [see Eq. (82)]. This compensates for the growth of the F_{mn} given in Table III with m for given n and suppresses the contribution from energetically close, lower-lying virtual states to the pole terms for given n of the reference state. We also observe the decreasing trend in the dipole matrix elements given in Table III with n for given m. However, it would be interesting to investigate if there is a further deeper reason for the apparent nonparametric (there is no factor of the fine-structure constant involved) suppression of the pole terms and mixing terms in long-range interactions involving higher excited states of simple atomic systems. This analysis is left for further study.

ACKNOWLEDGMENTS

This project was supported by the National Science Foundation (Grants No. PHY-1403973 and No. PHY-1710856) and by the Missouri Research Board. The high-precision experiments carried out at MPQ Garching under the guidance of Professor T. W. Hänsch have been a major motivation and inspiration for the current theoretical work. The authors also acknowledge helpful conversations with A. Matveev and N. Kolachevsky.

APPENDIX: DIPOLE MATRIX ELEMENTS F_{mn} AND H_{mn}

We are concerned with the evaluation of dipole matrix elements of bound-state Schrödinger hydrogen wave functions

$$G^{\ell_1\ell\ell_2}_{n_1 n n_2} = \langle n_1\ell_1 m_1|\vec{d}|n\ell m\rangle \cdot \langle n\ell m|\vec{d}|n_2\ell_2 m_2\rangle, \tag{A1}$$

where $\vec{d} = e\vec{r}$ is the dipole operator and the dimensionless dipole matrix elements F_{mn} and H_{mn} are given by

$$F_{mn} = \frac{G^{010}_{nmn}}{e^2 a_0^2}, \quad H_{mn} = \frac{G^{010}_{nm1}}{e^2 a_0^2}. \tag{A2}$$

The well-known expression for the radial function $R_{n\ell}(r)$,

$$R_{n\ell}(r) = \sqrt{\frac{(n-\ell-1)!}{(n+\ell)!}} \frac{2}{n^2 a_0^{3/2}} \left(\frac{2r}{a_0 n}\right)^{\ell} \exp\left(-\frac{r}{a_0 n}\right) L^{2\ell+1}_{n-\ell-1}\left(\frac{2r}{n a_0}\right), \tag{A3}$$

allows us to bring the dipole transition matrix element into the form

$$\begin{aligned}\int_0^\infty dr\, r^3 R_{n'\ell'}(r) R_{n\ell}(r) = {} & \sqrt{\frac{(n'-\ell'-1)!}{(n'+\ell')!}} \sqrt{\frac{(n-\ell-1)!}{(n+\ell)!}} \frac{a_0}{4 n^{\ell+2} n'^{\ell'+2}} \int_0^\infty dx\, x^{3+\ell+\ell'} \\ & \times \exp\left[-\frac{x}{2}\left(\frac{1}{n}+\frac{1}{n'}\right)\right] L^{2\ell'+1}_{n'-\ell'-1}\left(\frac{x}{n'}\right) L^{2\ell+1}_{n-\ell-1}\left(\frac{x}{n}\right),\end{aligned} \tag{A4}$$

where $x = 2r/a_0$. A result obtained for the radial matrix element in Ref. [24] is reproduced in Eq. (63.2) of Ref. [27]; the latter appears to benefit from some corrections for typographical errors that occurred in the original work [24]. Direct application of Eq. (63.2) of Ref. [27] leads to the formula

$$G^{010}_{n_1 n n_2} = (-1)^{n_1+n_2} \frac{16 n^5 n_1^{5/2} n_2^{5/2} (n^2-1) e^2 a_0^2}{(n-n_1)^4 (n-n_2)^4} \left(\frac{n-n_1}{n+n_1}\right)^{n+n_1} \left(\frac{n-n_2}{n+n_2}\right)^{n+n_2} T_1 T_2, \tag{A5a}$$

where

$$\begin{aligned} T_1 &= {}_2F_1(2-n,1-n_1,2,u_2) - \frac{(n-n_1)^2}{(n+n_1)^2} {}_2F_1(-n,1-n_1,2,u_2), \\ T_2 &= {}_2F_1(2-n,1-n_2,2,u_2) - \frac{(n-n_2)^2}{(n+n_2)^2} {}_2F_1(-n,1-n_2,2,u_2), \end{aligned} \tag{A5b}$$

and the arguments of the hypergeometric functions are

$$u_1 = -\frac{4 n n_1}{(n-n_1)^2}, \quad u_2 = -\frac{4 n n_2}{(n-n_2)^2}. \tag{A5c}$$

As it stands, formula (A5) is not applicable to the case $n = n'$ and has to be supplemented by the result

$$G^{010}_{nnn} = \tfrac{9}{4} n^2 (n^2-1) e^2 a_0^2. \tag{A6}$$

An alternative representation of the transition matrix elements that encompasses both formulas (A5) and (A6) would thus be desirable. However, a literature search including Sec. 2.19.4 of [28] does not reveal any immediately applicable integral formulas for integrals of the type (A4). However, an entry in a recently published online database [29] allows us to express the integral (A4) as a finite nested double sum over terms involving the Pochhammer symbol $(a)_n = \Gamma(a+n)/\Gamma(a)$,

$$\int_0^\infty dt\, t^{\alpha-1} \exp(-pt) L^{\lambda}_m(at) L^{\beta}_n(bt) = \frac{\Gamma(\alpha)(\lambda+1)_m (\beta+1)_n p^{-\alpha}}{m! n!} \sum_{j=0}^{m} \frac{(-m)_j (\alpha)_j}{j! (\lambda+1)_j} \left(\frac{a}{p}\right)^j \sum_{k=0}^{n} \frac{(-n)_k (j+\alpha)_k}{k! (\beta+1)_k} \left(\frac{b}{p}\right)^k. \tag{A7}$$

The inner sum can be expressed in terms of a terminating hypergeometric function. The coefficient $G^{010}_{n_1 n n_2}$ is finally written in a rather compact form as

$$\begin{aligned} G^{010}_{n_1 n n_2} = {} & e^2 a_0^2 2^{10} \frac{(n_1 n_2)^{7/2} n^5 (n^2-1)}{(n+n_1)^5 (n+n_2)^5} \sum_{\zeta=0}^{n_1-1} \frac{(1-n_1)_\zeta (5)_\zeta}{\zeta! (2)_\zeta} \left(\frac{2n}{n_1+n}\right)^\zeta {}_2F_1\left(2-n,5+\zeta,4,\frac{2n_1}{n+n_1}\right) \\ & \times \sum_{\beta=0}^{n_2-1} \frac{(1-n_2)_\beta (5)_\beta}{\beta! (2)_\beta} \left(\frac{2n}{n_2+n}\right)^\beta {}_2F_1\left(2-n,5+\beta,4,\frac{2n_2}{n+n_2}\right). \end{aligned} \tag{A8}$$

The case $n_1 = n_2 = n$, which is excluded from the treatment described in Ref. [24], is important in the derivation of Eq. (80).

[1] C. M. Adhikari, V. Debierre, A. Matveev, N. Kolachevsky, and U. D. Jentschura, Long-range interactions of hydrogen atoms in excited states. I. $2S$-$1S$ interactions and Dirac-δ perturbations, Phys. Rev. A **95**, 022703 (2017).

[2] H. Safari and M. R. Karimpour, Body-Assisted van der Waals Interaction between Excited Atoms, Phys. Rev. Lett. **114**, 013201 (2015).
[3] M. Donaire, R. Guérout, and A. Lambrecht, Quasiresonant van der Waals Interaction between Nonidentical Atoms, Phys. Rev. Lett. **115**, 033201 (2015).
[4] U. D. Jentschura, C. M. Adhikari, and V. Debierre, Virtual Resonant Emission and Long-Range Tails in van der Waals Interactions of Excited States: QED Treatment and Applications, Phys. Rev. Lett. **118**, 123001 (2017).
[5] M. I. Chibisov, Dispersion interaction of neutral atoms, Opt. Spectrosc. **32**, 1 (1972).
[6] W. J. Deal and R. H. Young, Long-range dispersion interactions involving excited atoms; the H(1s) − H(2s) interaction, Int. J. Quantum Chem. **7**, 877 (1973).
[7] A. Z. Tang and F. T. Chan, Dynamic multipole polarizability of atomic hydrogen, Phys. Rev. A **33**, 3671 (1986).
[8] U. D. Jentschura, V. Debierre, C. M. Adhikari, A. Matveev, and N. Kolachevsky, Long-range interactions of excited hydrogen atoms. II. Hyperfine-resolved 2S-2S system, Phys. Rev. A **95**, 022704 (2017).
[9] U. D. Jentschura and V. Debierre, Long-range tails in van der Waals interactions of excited-state and ground-state atoms, Phys. Rev. A **95**, 042506 (2017).
[10] U. Jentschura and K. Pachucki, Higher-order binding corrections to the Lamb shift of 2P states, Phys. Rev. A **54**, 1853 (1996).
[11] A. Czarnecki, U. D. Jentschura, and K. Pachucki, Calculation of the One- and Two-Loop Lamb Shift for Arbitrary Excited Hydrogenic States, Phys. Rev. Lett. **95**, 180404 (2005).
[12] K. Pachucki, Relativistic corrections to the long-range interaction between closed-shell atoms, Phys. Rev. A **72**, 062706 (2005).
[13] V. B. Berestetskii, E. M. Lifshitz, and L. P. Pitaevskii, *Quantum Electrodynamics*, 2nd ed., Course of Theoretical Physics Vol. 4 (Pergamon, Oxford, 1982).
[14] U. D. Jentschura, Corrections to Bethe logarithms induced by local potentials, J. Phys. A **36**, L229 (2003).
[15] U. D. Jentschura, S. Kotochigova, E.-O. Le Bigot, P. J. Mohr, and B. N. Taylor, Precise Calculation of Hydrogenic Energy Levels Using the Method of Least Squares, Phys. Rev. Lett. **95**, 163003 (2005).
[16] An interactive database of hydrogen and deuterium transition frequencies is available at http://physics.nist.gov/hdel.
[17] S. Salomonson and P. Öster, Solution of the pair equation using a finite discrete spectrum, Phys. Rev. A **40**, 5559 (1989).
[18] E. R. Switzer and C. M. Hirata, Phys. Rev. D **77**, 083006 (2008).
[19] J. Chluba and R. A. Sunyaev, Two-photon transitions in hydrogen and cosmological recombination, Astron. Astrophys. **480**, 629 (2008).
[20] C. W. Fabjan and F. M. Pipkin, Resonance narrowed Lamb shift measurement in hydrogen, Phys. Lett. A **36**, 69 (1971).
[21] H. Bateman, *Higher Transcendental Functions* (McGraw-Hill, New York, 1953), Vol. 1.
[22] H. Bateman, *Higher Transcendental Functions* (McGraw-Hill, New York, 1953), Vol. 2.
[23] S. Wolfram, *The Mathematica Book*, 4th ed. (Cambridge University Press, Cambridge, 1999).
[24] W. Gordon, Zur Berechnung der Matrizen beim Wasserstoffatom, Ann. Phys. (Leipzig) **394**, 1031 (1929).
[25] J. C. deVries, Ph.D. thesis, Massachusetts Institute of Technology, 2002, available at https://dspace.mit.edu/handle/1721.1/4108.
[26] T. Udem (private communication, 2017).
[27] H. A. Bethe and E. E. Salpeter, *Quantum Mechanics of One- and Two-Electron Atoms* (Springer, Berlin, 1957).
[28] A. P. Prudnikov, Y. A. Brychkov, and O. I. Marichev, *Integrals and Series, Volume II: Special Functions* (Taylor & Francis, London, 1998).
[29] See http://functions.wolfram.com/05.08.21.0009.01.